Geochimica et Cosmochimica Acta Vol. 56, pp. 587–596

0016-7037/92/$5.00 + .00

Dynamic model of oscillatory zoning of trace elements in calcite: Double layer, inhibition, and self-organization

YIFENG WANG and ENRIQUE MERINO
Department of Geological Sciences, Indiana University, Bloomington, IN 47405, USA

(*Received December* 11, 1990; *accepted in revised form November* 20, 1991)

Abstract—Calcite growing from an aqueous solution containing growth-inhibiting cations such as Mn^{2+} can acquire oscillatory zoning of trace elements by this feedback: The growth-induced H^+ buildup at the growth surface makes the surface more positive, thus preventing inhibiting cations from attaching to the growth sites and accelerating the growth rate. The increase in growth rate in turn further accelerates H^+ accumulation. This feedback is quantitatively modeled by a system of nonlinear differential equations that takes account of calcite growth, inhibition, diffusion, and mass continuity. For parameter values consistent with actual aqueous-ion diffusivities and concentrations in diagenetic waters, numerical solutions of the system of equations yield both oscillatory calcite growth and oscillatory concentration profiles of trace elements taken up by the calcite. The plausibility of the feedback makes it unnecessary to interpret oscillatory zoning of trace elements in calcite by calling on ad-hoc, large-scale, periodic changes in bulk water chemistry.

SYMBOLS

c_i	concentration of aqueous species i
$\bar{c}_i$	average concentration of species i within the boundary layer
c_i^0	concentration of species i next to the calcite growth surface
c_i^∞	concentration of species outside the boundary layer
D_i	diffusion coefficient of species i in the solution
K	equilibrium constants for reaction (1), Eqn. (2)
k	reaction rate constant for reaction (1), Eqns. (2–3)
K_1, K_2	equilibrium constants for reactions (5–6), respectively
k_1, k_2, k_1', k_2'	constants in Eqn. (A5)
L	boundary layer thickness
R	Reaction rate of reaction (1) (mol/cm^2 s)
S, D, Q	quantities that characterize the behavior of the linearized Eqn. (A4); defined in Eqn. (A7)
T	typical time, Eqn. 28
t	time
u, v	scaled concentrations of Ca^{2+} and H_2CO_3, respectively, next to the crystal surface
u_0, v_0	concentrations u and v at a steady state, respectively
W_1, W_2	reaction rates of reactions (5–6), respectively (mol/cm^3 s)
X	distance away from crystal surface
y	position of the growth surface with respect to the initial position, Eqn. (30)
α, β_1, β_2	constants (Eqn. 4) to adjust the ability of H^+ to reduce the inhibiting effect on calcite growth
γ	θ times the ratio of far-from-the-front concentrations of Ca^{2+} and H_2CO_3 (Eqn. 28)
δu, δv	small departures of u, v from their respective steady state values u_0, v_0
ζ, ζ_1, ζ_2	eigenvalues in Eqns. (A5–A6)
θ	ratio of diffusivities of Ca^{2+} and H_2CO_3
θ_c	critical value of θ, Eqn. (A10)
λ	scaled value of rate constant α
ρ	molar density of calcite
τ	scaled time
Φ, Ψ	defined as $du/d\tau$ and $dv/d\tau$, respectively

INTRODUCTION

CONCENTRIC ZONING OF TRACE elements in diagenetic calcite cements has been reported widely and interpreted as reflecting rapid and frequent changes in bulk fluid composition (MEYERS, 1974, 1978; GROVER and READ, 1983). This interpretation underlies so-called cement stratigraphy. It involves a large-scale cause to explain a small-scale effect; neglects the crucial detail that the concentric zoning is oscillatory, at least in some cases; and is inconsistent with the lack of correlation between specific zoning patterns for two nearby crystals in the same hand specimen (Fig. 1 and p. 222 in MASON, 1987). These problems have been pointed out by MASON (1987), REEDER (1986), and EMERY and MARSHALL (1989). The oscillatory, concentric zoning has a repeat distance ranging from <1 μm to tens of μm, and the amplitude of the oscillations in manganese (and other trace element) concentration is up to several hundred ppm (EMERY and MARSHALL, 1989; DROMGOOLE and WALTER, 1990a; FRASER et al., 1989; MASON, 1987; MEYERS et al., 1988; FAIRCHILD, 1983; FRANK et al., 1982; PIERSON, 1981; and references therein).

The experiments of FAGIOLI et al. (1985), TEN HAVE and HEIJNEN (1985), REEDER (1986), and REEDER et al. (1990), however, point to a completely different genesis of concentric, oscillatory zoning in calcite crystals: The zoning was produced not by changes in the starting bulk solution but by "periodic instabilities inherent to the growth process" (REEDER, 1986, p. 746).

REEDER (1986) proposed that the oscillatory zonation in calcite could be accounted for by self-organizational models similar to those of HAASE et al. (1980) and ALLÈGRE et al. (1981) for oscillatory zoning in plagioclase. These models, however, turn out not to be applicable to the case of interest here. The model proposed by HAASE et al. (1980) is based on a feedback which necessarily generates a complete (or at least very wide) range of solid solution. This mechanism cannot work where one component reaches only trace concentrations, as is the case for trace elements in calcite. This is because the multiple valuedness found by HASSE et al. (1980, Fig. 1) for the crystal-surface mole fraction of one component disappears as the solid solution becomes very dilute. The model proposed by ALLÈGRE et al. (1981) is based on arbitrarily imposing a delayed response of the growth rate to variations in the concentration of species in the liquid; but in the case of oscillatory zoning in calcite, we cannot see a priori what specific mechanism could cause that required delay.

Here we propose a feedback, and a dynamic model based on it, autonomously able to produce oscillatory zoning of trace elements in calcite without calling on repeated (and improbable) large-scale changes in bulk water chemistry. That is, the oscillatory zoning produced is self-organizational. Self-organization is the spontaneous patterning of a system through its own internal dynamics (NICOLIS and PRIGOGINE, 1977; MERINO, 1984; ORTOLEVA et al., 1987); it requires disequilibrium and feedback. The feedbaek we propose involves H^+ accumulation, surface adsorption, and calcite growth inhibition.

PROPOSED MECHANISM OF OSCILLATORY ZONING IN CALCITE

Chemical Reaction

We study calcite growth from supersaturated calcium carbonate solutions containing a cation inhibitor. At pH = 6–10, we regard Ca^{2+} and HCO_3^- as the main species supplying the necessary ions to the calcite crystal surface, according to:

$$Ca^{2+} + HCO_3^- \rightarrow CaCO_3(c) + H^+, \qquad (1)$$

which is consistent with experiments of calcite dissolution (PLUMMER et al., 1978). Upon calcite growth, reaction (1) releases H^+, which accumulates at the growth surface if the reaction rate is fast enough relative to diffusion of aqueous ions. The rate of reaction (1), R, can be written as

$$R = k\left(c^0_{Ca^{2+}} c^0_{HCO_3^-} - \frac{c^0_{H^+}}{K}\right), \qquad (2)$$

where k is the rate constant; c_i^0 is the concentration of species i next to the crystal surface, and K is the equilibrium constant of reaction (1). For a sufficiently supersaturated (or far from equilibrium) system, the forward reaction predominates, and Eqn. (2) simplifies to

$$R = k c^0_{Ca^{2+}} c^0_{HCO_3^-}. \qquad (3)$$

This rate law is the same one proposed by PLUMMER et al. (1978, last term in Eqn. 6). Eqn. (3) indicates that far from equilibrium, H^+ cannot affect the rate, except possibly through modifying the rate constant, k.

Inhibitors

Attachment of species to crystal surfaces may markedly accelerate or inhibit the rate of mineral dissolution and growth (HELGESON et al., 1984; BLUM and LASAGA, 1988; CARROLL-WEBB and WALTHER, 1988; STUMM et al., 1983; STUMM and WIELAND, 1990; DROMGOOLE and WALTER, 1990b; and references therein). The inhibition of calcite growth rates by many cations, including Mn^{2+}, Fe^{2+}, and Zn^{2+}, has been studied by MEYER (1984), and DROMGOOLE and WALTER (1990b) have studied inhibition by Mn^{2+} in detail. The strength of the inhibition depends on the identity of the inhibitor, its concentration, initial growth rate (the rate without inhibitors), interference by other inhibitors, thermodynamic stability of the solid solution, and other factors. The inhibitor works by blocking kinks (MEYER, 1984).

Double Layer and Adsorption

Electrical charge at the crystal/solution interface gives rise to an electrical double layer in the aqueous solution next to the crystal surface. The surface charge usually depends on the concentrations of potential-determining ions. Possible potential-determining ions for calcite surface charge are H^+, OH^-, H_2CO_3, HCO_3^-, CO_3^{2-}, Ca^{2+}, and $CaOH^+$ (PARKS, 1975; STUMM and MORGAN, 1981, p. 631). Of all these, we retain here for simplicity only H^+, because HCO_3^- is by assumption very high (and approximately constant); and as H^+ increases, all the other species next to the crystal surface change in the direction of making the crystal surface also more positive, just as H^+ does.

The surface charge of calcite significantly depends on pH only in the intermediate pH range (6–10), and its isoelectric point (iep) is about 8.3 (STUMM and MORGAN, 1981, Fig. 10.3). Because this pH range approximately coincides with that for many natural waters, it follows that calcite growth can modify its own electrical double-layer by H^+ accumulation next to the crystal surface.

In turn, the adsorption of species on a mineral surface depends on surface charge, itself determined mainly by H^+. If the pH decreases below the isoelectric point (iep), surface charge becomes positive, cation adsorption drops (because of increased repulsion), and anion adsorption increases (DREVER, 1988, p. 88). If one of the cations adsorbed on calcite inhibits crystal growth, then an increase in H^+ concentration reduces the strength of the inhibition, which allows the calcite growth rate to increase. At the same time, the drop in cation adsorption would presumably lead to a drop in cation incorporation into calcite. In short, calcite-growth-driven H^+ accumulation at the crystal surface both enhances the growth rate (by modifying through inhibition the reaction rate constant k in Eqn. 3) and causes the amount of incorporated trace elements to decrease.

Oscillatory Mechanism

The above leads to a self-organizational feedback for oscillatory zoning in calcite. The feedback is illustrated in Fig. 1a. Assume that the solution in the system is highly supersaturated with calcite. Assume that the solution initially contains Mn^{2+} (or other inhibiting cations), and calcite starts

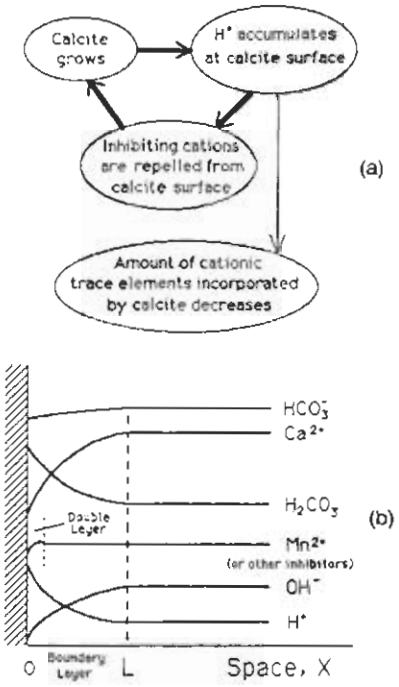

FIG. 1. (a) Feedback proposed for oscillatory calcite growth and oscillatory trace element incorporation. (b) Model system showing schematic concentrations of relevant aqueous species vs. distance from the calcite crystal surface, taken as origin. The calcite surface moves to the right. The thickness L of the boundary layer is probably of order 0.01–1 mm; that of the double layer is of order 1–10 nm (PARKS, 1975). Upon calcite growth, H^+ and H_2CO_3 accumulate at the crystallization front. The feedback in Fig. 1a among growth rate, surface charge, and strength of inhibition can produce oscillatory zoning of trace elements in the calcite crystal.

crystallization at a pH > iep. At the initial pH, the growth rate is low because, the surface charge being negative, Mn^{2+} is easily adsorbed on growth sites (kinks). But as crystal growth proceeds by breakdown of HCO_3^- according to reaction (1), H^+ accumulates at the surface. Surface charge becomes more positive, thus increasingly repelling Mn^{2+} away from the surface itself. Since Mn^{2+} is an inhibitor, keeping it away increases calcite growth rate; this increase, in turn, accelerates H^+ accumulation. This positive feedback makes the calcite grow so fast that Ca^{2+} concentration becomes depressed next to the growth surface, eventually becoming so low at the growth front that growth slows down, and H^+ accumulation at the surface decreases, for H^+ can now efficiently diffuse away (via H_2CO_3). Then crystal growth becomes even slower because, with the crystal surface being now less positive (or even negative), Mn^{2+} can easily attach on the surface again. When the growth rate is so low that Ca^{2+} can recover, another growth cycle is triggered. The feedback can be regarded as a kind of H^+ autocatalysis that works only if a cation inhibitor is present.

Crucial to the feedback is the assumption that the system is far from equilibrium. Because of it, H^+ has a negligible effect on the affinity term of the reaction rate and it affects only the constant, k, in Eqn. (3). Also because of it, we can neglect the double layer effect on the adsorption of Ca^{2+} but not on the adsorption of inhibiting cations in trace concentrations. Indeed, the double layer, when it is positive, does try to repel both Ca^{2+} and the inhibiting cations; but while for Ca^{2+} the chemical potential in favor of adsorption vastly overpowers the electrostatic potential against it (STUMM and MORGAN, 1981, Eqn. 24, p. 622), for the low-concentration inhibitors, the two terms are of the same order, and neither one can be neglected.

To complete the basic framework of the model, we now need to incorporate the inhibiting effect into the rate constant, k, of Eqn. (3). The inhibiting effect is controlled (through the repulsion by the double layer) by the H^+ concentration, as we have discussed above, and by inhibitor concentration in the aqueous solution. For mathematical simplicity, we assume here that this latter concentration remains constant next to the crystal's surface (this removes a differential equation from the system below), an assumption made plausible within the context of the model because when calcite growth rate increases, relatively less manganese is incorporated into calcite. This simplification leaves the rate constant, k, in Eqn. (3) controlled only by H^+ concentration at the crystal surface. We thus express k as a monotonically increasing function of the scaled H^+ concentration, defined as $(c^0_{H^+} - c^\infty_{H^+})/c^\infty_{H^+}$:

$$k = \alpha\left[1 + \beta_1 \frac{c^0_{H^+} - c^\infty_{H^+}}{c^\infty_{H^+}} + \beta_2\left(\frac{c^0_{H^+} - c^\infty_{H^+}}{c^\infty_{H^+}}\right)^2\right], \quad (4)$$

where $c^\infty_{H^+}$ is the H^+ concentration far away from the crystallization surface, and α, β_1, and β_2 are positive constants. The quadratic term in Eqn. (4) allows the feedback to be strong.

CRYSTALLIZATION MODEL

The model system (Fig. 1b) contains the aqueous species H_2CO_3, HCO_3^-, Ca^{2+}, H^+, OH^-, and Mn^{2+}. Besides reaction (1), the system includes the two aqueous reactions:

$$HCO_3^- + H^+ = H_2CO_3, \quad \text{and} \quad (5)$$

$$H^+ + OH^- = H_2O, \quad (6)$$

with rates W_1 and W_2, respectively. The continuity equation for each relevant species in the region ahead of the crystal surface, $X > 0$, is:

$$\frac{\partial c_{HCO_3^-}}{\partial t} = D_{HCO_3^-}\frac{\partial^2 c_{HCO_3^-}}{\partial X^2} - W_1, \quad (7)$$

$$\frac{\partial c_{Ca^{2+}}}{\partial t} = D_{Ca^{2+}}\frac{\partial^2 c_{Ca^{2+}}}{\partial X^2}, \quad (8)$$

$$\frac{\partial c_{H_2CO_3}}{\partial t} = D_{H_2CO_3}\frac{\partial^2 c_{H_2CO_3}}{\partial X^2} + W_1, \quad (9)$$

$$\frac{\partial c_{H^+}}{\partial t} = D_{H^+}\frac{\partial^2 c_{H^+}}{\partial X^2} - W_1 - W_2, \quad \text{and} \quad (10)$$

$$\frac{\partial c_{OH^-}}{\partial t} = D_{OH^-}\frac{\partial^2 c_{OH^-}}{\partial X^2} - W_2. \quad (11)$$

Second, we write mass balance equations at the crystal surface, $X = 0$:

$$R = -D_{H_2CO_3}\frac{\partial c_{H_2CO_3}}{\partial X} - D_{H^+}\frac{\partial c_{H^+}}{\partial X} + D_{OH^-}\frac{\partial c_{OH^-}}{\partial X}, \quad (12)$$

$$R = D_{Ca^{2+}} \frac{\partial c_{Ca^{2+}}}{\partial X}, \quad \text{and} \tag{13}$$

$$R = D_{HCO_3^-} \frac{\partial c_{HCO_3^-}}{\partial X} + D_{H_2CO_3} \frac{\partial c_{H_2CO_3}}{\partial X}, \tag{14}$$

where t is time, X is the distance from the crystal surface, R is the calcite growth rate, and D_i is the diffusion coefficient of the ith aqueous species ($i = H_2CO_3$, Ca^{2+}, HCO_3^-, H^+, and OH^-).

The above system of equations can be simplified because the homogeneous reactions (5–6) are fast compared with the heterogeneous reaction (1). Thus, W_1 and W_2 can be eliminated in Eqns. (7–11) by taking reaction (5–6) to be in equilibrium (ORTOLEVA et al., 1987, pp. 1001–1002). Also, because the pH for the system of interest is 6.5–9.5 and the solution is highly supersaturated with calcite, it usually holds that $c_{HCO_3^-} \gg c_{H_2CO_3}$, $c_{H_2CO_3} \gg c_{H^+}$, $c_{H_2CO_3} \gg c_{OH^-}$ and $c_{HCO_3^-} \gg c_{Ca^{++}}$. The simplified system of equations thus becomes for $X > 0$:

$$\frac{\partial c_{Ca^{2+}}}{\partial t} = D_{Ca^{2+}} \frac{\partial^2 c_{Ca^{2+}}}{\partial X^2}, \tag{15}$$

$$\frac{\partial c_{H_2CO_3}}{\partial t} = D_{H_2CO_3} \frac{\partial^2 c_{H_2CO_3}}{\partial X^2}, \tag{16}$$

$$c_{HCO_3^-} = \text{constant} = c^{\infty}_{HCO_3^-}, \tag{17}$$

$$c_{H^+} = c_{H_2CO_3} / K_1 c^{\infty}_{HCO_3^-}, \quad \text{and} \tag{18}$$

$$c_{OH^-} = K_2 / c_{H^+}. \tag{19}$$

For $X = 0$:

$$R = D_{Ca^{2+}} \frac{\partial c_{Ca^{2+}}}{\partial X}, \quad \text{and} \tag{20}$$

$$R = -D_{H_2CO_3} \frac{\partial c_{H_2CO_3}}{\partial X}, \tag{21}$$

where K_1 and K_2 are the equilibrium constants of reactions (5, 6), respectively. Because the last two terms of Eqn. 12 are negligible with respect to the first term on the right, H^+'s released at the growth surface by reaction (1) diffuse away from it mainly in the form of H_2CO_3, and Eqn. (12) yields Eqn. (21). Combining Eqns. (3, 4, 17, and 18), the reaction rate becomes:

$$R = \alpha c^{\infty}_{HCO_3^-} \left[1 + \beta_1 \frac{c^0_{H_2CO_3} - c^{\infty}_{H_2CO_3}}{c^{\infty}_{H_2CO_3}} + \beta_2 \left(\frac{c^0_{H_2CO_3} - c^{\infty}_{H_2CO_3}}{c^{\infty}_{H_2CO_3}} \right)^2 \right] c^0_{Ca^{2+}}. \tag{22}$$

We now see that the system can be described by only two independent variables, $c_{Ca^{++}}$ and $c_{H_2CO_3}$. Equations (15, 16, and 20–22) form a closed system. The inhibiting cations, such as Mn^{2+}, are implicitly included in Eqn. (22). It is because of the inhibiting effect that the rate constant can be expressed in terms of c_{H^+} (Eqn. 4), which is in turn determined by $c_{H_2CO_3}$ (Eqn. 18).

To further simplify Eqns. (15–22), we now focus on the boundary layer, defined as the distance at which concentrations of relevant species first reach their far-away values. By integrating both sides of (15 and 16) over the width L of the boundary layer, we obtain:

$$L \frac{d\bar{c}_{Ca^{2+}}}{dt} = D_{Ca^{2+}} \left. \frac{\partial c_{Ca^{2+}}}{\partial X} \right|_{X=L} - R, \quad \text{and} \tag{23}$$

$$L \frac{d\bar{c}_{H_2CO_3}}{dt} = D_{H_2CO_3} \left. \frac{\partial c_{H_2CO_3}}{\partial X} \right|_{X=L} + R, \tag{24}$$

where

$$\bar{c}_i = \frac{1}{L} \int_0^L c_i \, dX, \quad i = Ca^{2+}, H_2CO_3. \tag{25}$$

Using the approximation,

$$\bar{c}_i = \frac{c_i^0 + c_i^{\infty}}{2}, \quad i = Ca^{2+}, H_2CO_3, \quad \text{and} \tag{26}$$

$$\left. \frac{\partial c_i}{\partial X} \right|_{X=L} = \frac{c_i^{\infty} - c_i^0}{L}, \quad i = Ca^{2+}, H_2CO_3, \tag{27}$$

and scaling variables according to

$$u = \frac{c^0_{Ca^{2+}}}{c^{\infty}_{Ca^{2+}}}, \quad v = \frac{c^0_{H_2CO_3} - c^{\infty}_{H_2CO_3}}{c^{\infty}_{H_2CO_3}},$$

$$\tau = \frac{t}{T}, \quad T = \frac{L}{2D_{Ca^{2+}}}, \quad \text{and}$$

$$\lambda = \frac{\alpha c^{\infty}_{HCO_3^-} L}{D_{Ca^{2+}}}, \quad \theta = \frac{D_{Ca^{2+}}}{D_{H_2CO_3}}, \quad \gamma = \frac{D_{Ca^{2+}} c^{\infty}_{Ca^{2+}}}{D_{H_2CO_3} c^{\infty}_{H_2CO_3}}, \tag{28}$$

we have

$$\frac{du}{d\tau} = 1 - u - \lambda(1 + \beta_1 v + \beta_2 v^2)u, \quad \text{and} \tag{29a}$$

$$\theta \frac{dv}{d\tau} = -v + \gamma\lambda(1 + \beta_1 v + \beta_2 v^2)u. \tag{29b}$$

This is the simplest system that represents the evolution of the concentrations of Ca^{2+} and H_2CO_3 at the calcite growth surface, including the feedback qualitatively described above. This system of equations is similar to that describing agate crystallization (WANG and MERINO, 1990).

AUTONOMOUS OSCILLATION OF CALCITE GROWTH

The problem of whether calcite growth can, through the feedback outlined above, autonomously oscillate with time reduces to finding the conditions under which Eqns. (29a and b) have oscillatory solutions. This is accomplished by finding the steady-state solutions to Eqns. (29a and b), carrying out a linear instability analysis, and solving numerically the full nonlinear system of Eqns. (29a and b).

Steady States and Linear Instability Analysis

The several possible steady states of the system of Eqns. (29a and b) are obtained in the Appendix. The linear instability analysis, also in the Appendix, reveals the behavior of the system around each steady state and provides ranges of

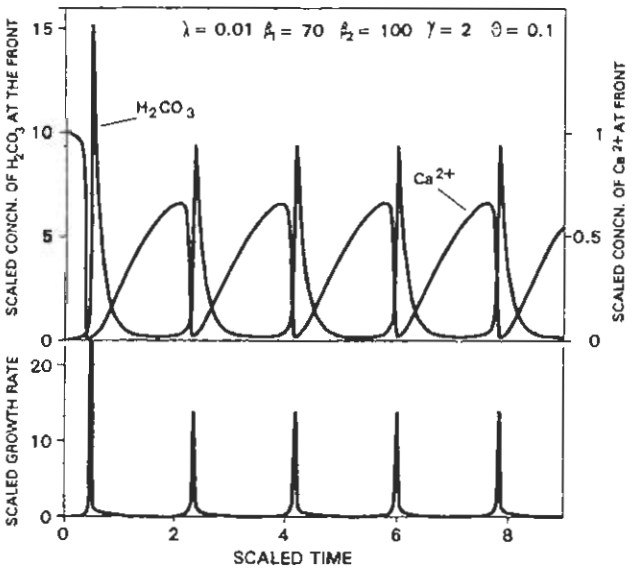

FIG. 2. Top two curves are scaled concentrations of H_2CO_3 and Ca^{2+} next to the calcite surface vs. time, calculated with Eqns. (29a and b). The bottom curve is the scaled growth rate of calcite vs. time. Parameter values used in the calculation are indicated and satisfy conditions obtained from a linear instability analysis (Appendix).

parameter values with which to carry out the numerical solutions. The steady states, named according to the behavior of the system around them, are saddle point, node (stable and unstable), and focus (stable and unstable). All these behaviors are discussed later in the section on behavior diagrams. The focus and unstable node are the ones of interest here, for they may produce oscillatory solutions.

Numerical Solutions

The full nonlinear system (29) has been solved numerically by a backward finite difference and Newton-Raphson methods. Using the criteria obtained by linear stability analysis to choose values for λ, γ, β_1, β_2, and θ (see Appendix), we find that there are indeed oscillatory solutions to Eqns. (29a and b). One set of solutions is shown in Fig. 2 for the indicated choices of parameters. The upper two curves in the figure show Ca^{2+} and H_2CO_3 concentrations at the growth surface vs. time since the start of the process. The scaled growth rate is given by the lower curve, which is calculated with Eqn. 22. Note that a time delay exists between the growth rate and Ca^{2+} concentration. This delay was artificially imposed in other problems of oscillatory crystallization (SAMOYLOVICH, 1979; ALLÈGRE et al., 1981), but our model brings it about naturally.

The position, y, of the growth surface with respect to the initial position is calculated with,

$$y = \frac{c^{\infty}_{Ca^{2+}} L}{\rho} \int_0^{\tau} \lambda(1 + \beta_1 v_0 + \beta_2 v_0^2) u d\tau, \qquad (30)$$

where ρ is the molar density of calcite. The concentrations of Ca^{2+} and H_2CO_3 and the growth rate can then be recalculated as functions of y. These profiles are shown in Fig. 3. Each band in the calcite crystal corresponds to one oscillation cycle of the concentrations; for the parameter values used, Figs. 2 and 3 show that band spacing equals 0.005 times the boundary layer thickness, L. In general, the spacing is probably between 10^{-3} and 10^{-2} length units of L.

From the concentrations of bicarbonate and carbonic acid given in Fig. 3, one can calculate the pH oscillations at the

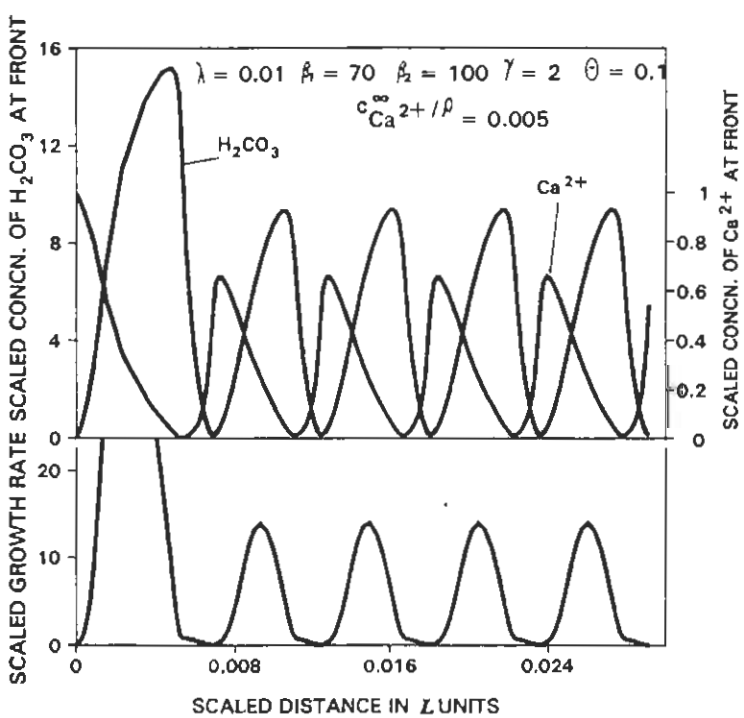

FIG. 3. Same concentrations and growth rate as in Fig. 2, but here vs. front position, y, which is obtained by integration of the growth rate (Eqn. 30).

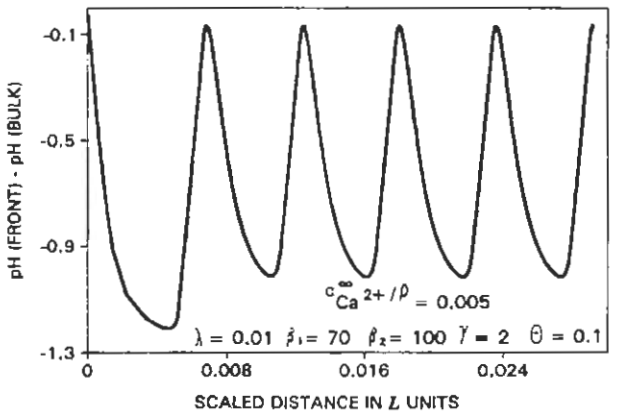

FIG. 4. pH at the crystal surface (evaluated with Eqn. (18), together with H_2CO_3 concentrations in Fig. 3) vs. front position. The quantity given along the ordinates is actually the departure of pH from the pH of the bulk solution. Parameter values as in Fig. 3. Because amount of trace elements adsorbed (and then incorporated) depends on pH at the growth front, oscillatory pH produces the oscillatory zoning of trace elements in calcite crystals.

crystal surface; these are shown in Fig. 4, where one can see that calculated pH fluctuations at the growth surface are of about one unit.

The numerical simulation also shows that the amplitude of the trace element oscillations increases with $\theta_c - \theta$. θ is the ratio of diffusivities of Ca^{2+} and H_2CO_3; θ_c is the critical value of θ, which is a function of λ, γ, β_1, and β_2 (see Appendix, Eqn. A10). For some values of $\theta_c - \theta$, the system displays transitional oscillation behaviors. Fig. 5a shows the case where the system oscillatorily approaches a steady state; Fig. 5b is for a system that shifts oscillatorily from an unstable steady state to a stable one. These various behaviors can probably all take place in calcite crystallization, yielding the wide variety of concentric zoning patterns reported.

BEHAVIOR DIAGRAM

Various types of behaviors of the system can be described by behavior diagrams in terms of the parameters λ, γ, β_1, β_2, and θ in the dynamic Eqns. (29a and b). Each type of behavior is separated from the others by boundaries, shown

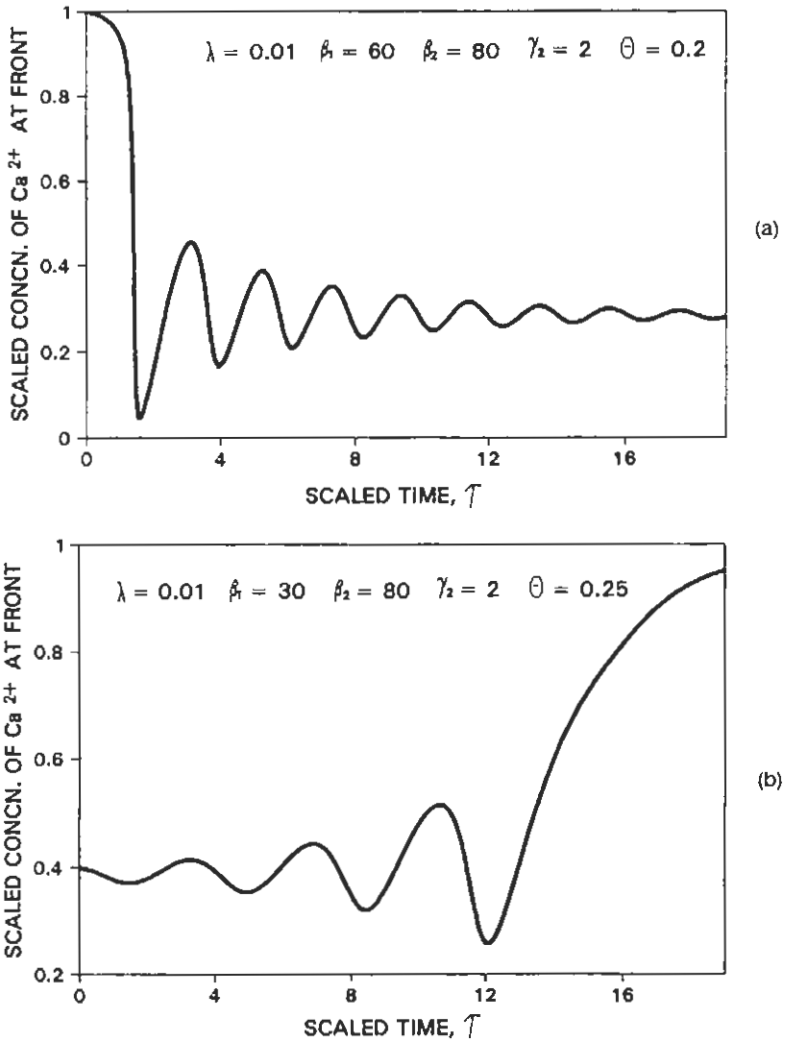

FIG. 5. (a) The system approaches a stable focus with an attenuated amplitude. (b) The system moves away oscillatorily from an unstable focus to a stable node. See classification of steady states in Appendix.

in Fig. 6. These boundaries are obtained from Eqns. (A8–A10) (see Appendix). Full nonlinear effects are taken into account by solving numerically the nonlinear Eqns. (29a and b) for sets of parameter values that correspond to each region of Fig. 6. Usually, the nonlinear effects stabilize the system when it is too far from a steady state. Consider first the case where the system has only one steady state (see Fig. 7). In this case, only focus or node (see the three types of steady state in Appendix) can exist, i.e., $S < 0$. For $\theta < \theta_c$, the focus or node is unstable, and the system moves away from the

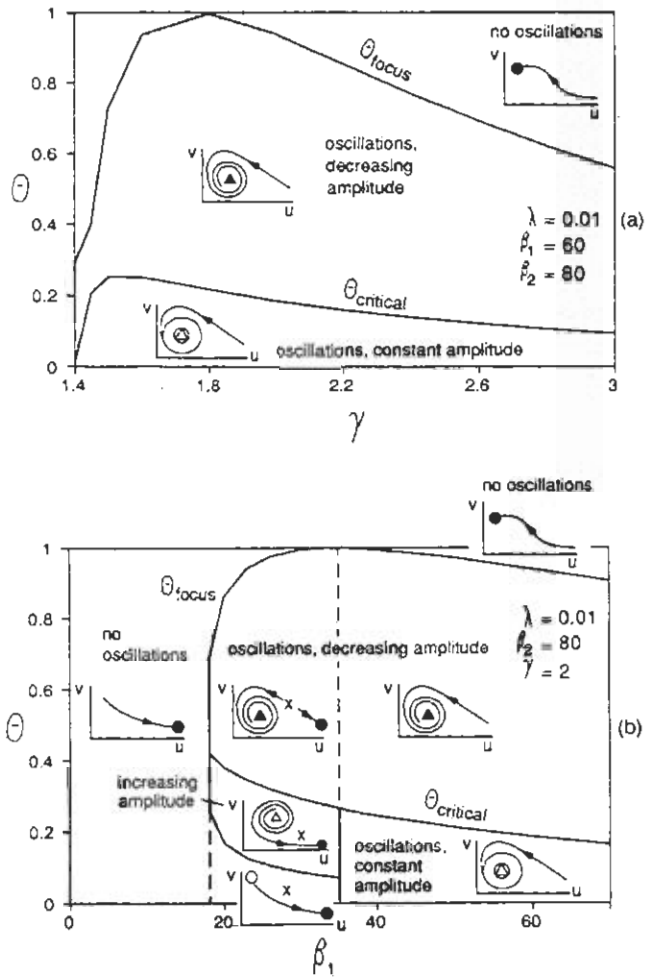

FIG. 6. Behavior diagrams for oscillatory calcite crystallization in parameter space (see text). Four behaviors are possible: No oscillation, oscillation with decreasing amplitude, oscillation with increasing amplitude, and oscillation with constant amplitude. Each behavior is associated with a different type of steady state: ×, saddle; ●, stable node; ○, unstable node; ▲, stable focus; △, unstable focus; and ◎, unstable focus or node. The behavior regions are separated by solid lines, which are determined by linear instability analysis (Appendix) and numerical simulation. A dashed line indicates that the regions on either side have same behaviors but different numbers of steady states. The $\theta_{critical}$ curve is calculated with Eqn. (A10) for a steady state; below it, the system is unstable around the steady state. The θ_{focus} curve (obtained with Eqn. (A9), Appendix) separates the region with focus from the region with nodes. Inside each region, a cartoon shows the corresponding type of variation of u and v (concentrations of Ca^{2+} and H_2CO_3) and the type of steady state. Replacing γ with λ or β_2 in Fig. 6(a) does not change the figure topology.

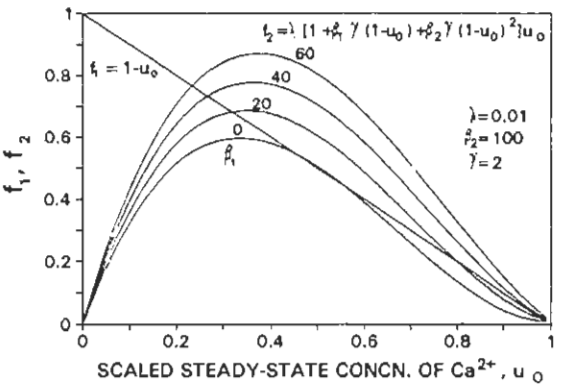

FIG. 7. Steady states are found by solving Eqn. (A1) by intersection of two functions, f_1 and f_2. Three steady states may coexist within a certain β_1 range; one of them, with intermediate concentrations, is a saddle point and is always unstable.

steady state; when it is far enough from it, the system becomes stabilized by the nonlinear effect, thus behaving only as a limit cycle—the system oscillates with a constant amplitude (see Fig. 2). For $\theta > \theta_c$ and $D < 0$, the steady state is a stable focus; hence the system, initially away from the steady state, oscillatorily approaches it (see Fig. 5a).

Where the system has three steady states, its behavior becomes more complex. Of the three (see Fig. 7), the one with intermediate Ca^{2+} concentration, state 2, is always a saddle point; the one with the highest concentration, state 3, is always a stable focus or node. Because its θ_c is negative, state 3 strongly attracts the system toward itself, and it behaves as a stable node. State 1, the one with the lowest Ca^{2+} concentration, can be either node or focus. When it is a node, the system cannot oscillate regardless of whether $\theta < \theta_c$ or not. When it is a focus, the system may behave as shown in Fig. 5a if $\theta > \theta_c$, or oscillatorily shift from state 1 to 3 if $\theta < \theta_c$ (Fig. 5b).

From the above discussion and the numerical simulation, we can construct the behavior diagram for the system. Fig. 6 shows two views of parameter space for indicated parameter values. The figure shows that the system can shift from one behavior domain to another by changes in the parameter values. In nature, these parameters are actually controlled by, for example, composition of pore solutions, fluid circulation, temperature, pressure, other mineral reactions adjacent to the growing calcite crystal, decomposition of organic matter, etc; also, these factors themselves naturally evolve with time. This is probably why various zoning patterns are often observed in calcite crystals.

From the two behavior diagrams in Fig. 6, and two more not shown here but very similar to Fig. 6a, we deduce the following approximate parameter ranges within which calcite can incorporate oscillatory concentrations of trace elements: $\lambda > 0.0065$, $\gamma > 1.4$, $\beta_1 > 18$, $\beta_2 > 8$, $\theta < 1$. The range predicted for θ is reasonable because the diffusivity for aqueous Ca^{2+} (which is charged) is indeed less than that for H_2CO_3 (which is neutral); see LI and GREGORY (1974). The range predicted for γ is also reasonable for many diagenetic waters, for which typically $c_{Ca^{2+}}/c_{H_2CO_3} > 10$; see, for example, MERINO (1979), Table 3.

DISCUSSION

The quantitative dynamical model proposed links inhibition of calcite growth, effect of the double layer on the adsorption of inhibitors, and far-from-equilibrium thermodynamics. It explores the idea that oscillatory zoning of trace elements in calcite crystals can be self-organizational. Assuming that calcite crystallizes from a supersaturated solution containing Mn^{2+} (or other cation inhibitors), the proposed positive feedback operates as follows (Fig. 1a): Upon calcite growth, H^+ accumulates at the growth surface; surface charge becomes more positive and repels the inhibitor; this causes the growth rate to go up, in turn further enhancing the accumulation of H^+. A linear stability analysis and numerical solutions of the full, nonlinear system of equations show that this feedback can indeed give rise to oscillatory crystallization of calcite. Assuming that the amount of a trace element incorporated into calcite is proportional to the amount of that trace element adsorbed on the growth surface, the oscillatory variation of pH at the growth surface (Fig. 4) leads to an oscillatory variation of the concentrations of trace elements incorporated into calcite. According to the model, all aqueous cationic trace elements, such as manganese and iron, should be incorporated in calcite more or less sympathetically, but cannot vary antipathetically. The reason for this is that adsorption-vs.-pH curves for cations display similar trends but are offset (Fig. 7 in YASUNAGA and IKEDA, 1986). This prediction agrees with observations by MASON (1987, Figs. 3–7) and FRASER et al. (1989, Fig. 4).

The model predicts (Fig. 3) that the spacing between bands is probably between 10^{-3} and 10^{-2} of the boundary layer thickness. The predicted spacing coincides in order of magnitude with observed spacings (REEDER, 1986; EMERY and MARSHALL, 1989) if L is chosen to be 0.01–1 mm, values that appear reasonable. According to Eqn. (30), the wavelength of the trace element oscillations is proportional to the supersaturation with respect to calcite (actually, to the ratio $c^{\infty}_{Ca^{2+}}/\rho$). Indeed, the supersaturation can range over a wide interval in nature, and so does the observed wavelength (which ranges from less than 1 μm to tens of μm). Similarly (Fig. 2), each band is seen to form in about two scaled time units, equivalent to several hours.

The predicted pH fluctuation at the crystal surface is about one unit (Fig. 4), which agrees well with the experimentally determined 1–2 pH units needed to change adsorption efficiency from 0 to 100% (HAYES and LECKIE, 1986; HONEYMAN and LECKIE, 1986; YASUNAGA and IKEDA, 1986; DAVIES, 1986.

The model proposed can produce very limited ranges of solid solution, as needed for the case of manganese oscillatory zoning in calcite. In contrast, models of the type proposed for plagioclase oscillatory zoning by HAASE et al. (1980) are based on mechanisms that necessarily yield very large (even complete) solid solution ranges and thus cannot, we think, apply to oscillations of trace elements.

The theoretical and experimental possibility that the trace element zoning in calcite results from the very dynamics of the growth process makes it unnecessary to interpret such zoning as caused by postulated large-scale changes in the bulk fluid, as done by MEYERS (1974) and GROVER and READ (1983). If the model proposed here is accurate, a set of oscillatory manganese bands in a calcite crystal suggests that the local system was highly supersaturated with respect to calcite, that the local pH was within one unit of the isoelectric point, and that cation inhibition took place. Inhibition by anions (such as phosphate, MEYER, 1984) would not permit a positive feedback, necessary for the mechanism proposed here. This points to a possible experimental test of the model: Add an inhibiting anion, such as phosphate, to a calcite growth experiment initially containing Mn^{2+} and see whether the ability to produce oscillations then disappears.

The behavior diagrams of Fig. 6 suggest that different types of banding patterns are produced in different regions of parameter space. Changes in parameter values can take place naturally through variations in temperature, bulk solution chemistry, etc. Specific oscillatory sequences, if found, could be interpreted in terms of specific ranges of values of some of the parameters in the theory, in accordance with Fig. 6. For example, a zoning sequence of decreasing amplitude (Fig. 5a) would imply that θ (the ratio of diffusion coefficients, Eqn. 28) was $> \theta_{critical}$ (region labelled "decreasing amplitude" on Fig. 6).

Since seawater contains on the order of 10^{-9} M of manganese and 10^{-8} M of iron (DREVER, 1988, p. 266), less than MEYER'S (1984) experimentally determined inhibiting concentrations, we think that the oscillating mechanism should not work for calcite grown from seawater. But we expect that oscillatorily zoned calcite is likely to form during diagenesis of sediments because pore solutions may become highly supersaturated with respect to calcite, and because Mn^{2+} (or Fe^{2+}) concentration can become high in the porewater (see also the end of the section on behavior diagrams).

Because a major element of the mechanism proposed is the electrostatic repulsion of aqueous cations by the double layer, uptake of different cations by a calcite crystal should vary in the same direction when passing from one sector to another, which it does (REEDER and GRAMS, 1987, Fig. 2). The mechanism might also have some bearing on the origin of sector zoning* because the intensity of the double layer effect on inhibitors (and catalysts) is bound to depend on the identity of each crystal face, as each of these should have its own iep and adsorption capacity. For the same reason, the model might explain the effect, if any, of a given inhibitor on crystal habit.

The model's basic idea that the accumulation of H^+ at the calcite surface can reduce the inhibiting effect is consistent with experimental observations that the partition coefficient of manganese between calcite and solution decreases with increasing calcite growth rate (LORENS, 1981; MUCCI, 1988; PINGITORE et al., 1988; DROMGOOLE and WALTER, 1990a). The model predicts correctly the dependence of inhibition strength on initial growth rate (i.e., rate without inhibitors) determined by MEYER (1984, Fig. 1), for both cation and anion inhibitors: Indeed, for a high initial growth rate, H^+ concentration at the crystal surface would be high enough to favor considerable repulsion of inhibiting cations and thus

* Among other minerals that crystallize from aqueous solutions, sector zoning occurs in calcite (REEDER and GRAMS, 1987), skarn garnets (FRAGA et al., 1982), and quartz (CHERNOV, 1984, p. 171).

little inhibition, whereas low initial rates would encourage less repulsion of cations and greater inhibition, for a given concentration of inhibitor. For anionic inhibitors, the relations predicted are exactly reversed. All these predictions are precisely as shown experimentally by MEYER (1984, Fig. 1).

The feedback proposed could also account for oscillatory pH changes observed during silicate dissolution (KUANG, 1989). Observed oscillatory zoning of aluminum in quartz overgrowths (HENRY et al., 1986; and STEPHEN G. FRANKS, ARCO Oil and Gas Company, pers. comm., 1990) is probably produced by an autocatalytic feedback (described in WANG and MERINO, 1990) similar to the one proposed here for calcite oscillatory zoning.

Acknowledgments—We thank the NSF Div. of Earth Sciences for support through grants EAR-9003633 and -9104198, the Exchange Program between Nanjiing and Indiana Universities for a fellowship, R. Hill of Indiana University for help, and R. A. Mason and S. A. Carroll for their incisive suggestions.

Editorial handling: R. A. Schmitt

REFERENCES

ALLÈGRE, C. J., PROVOST A., and JAUPART C. (1981) Oscillatory zoning: A pathological case of crystal growth. *Nature* **294**, 223–228.

BLUM A. and LASAGA A. (1988) Role of surface speciation in the low temperature dissolution of minerals. *Nature* **331**, 431–433.

CARROLL-WEBB S. A. and WALTHER J. V. (1988) A surface complex reaction model for the pH-dependence of corundum and kaolinite dissolution rates. *Geochim. Cosmochim. Acta* **52**, 2609–2623.

CHERNOV A. A. (1984) *Modern Crystallography III Crystal Growth*. Springer-Verlag.

COOK P. A. (1986) *Nonlinear Dynamical Systems*. Prentice-Hall.

DAVIES S. H. R. (1986) Mn(II) oxidation in the presence of lepidocrocite: The influence of other ions. In *Geochemical Processes at Mineral Surfaces* (ed. J. A. DAVIS and K. F. HAYES) pp. 487-502. American Chemical Society.

DREVER, J. I. (1988) *The Geochemistry of Natural Waters*. Prentice-Hall.

DROMGOOLE E. L. and WALTER L. M. (1990a) Iron and manganese incorporation into calcite: Effects of growth kinetics, temperature and solution chemistry. *Chem. Geol.* **81**, 311–336.

DROMGOOLE E. L. and WALTER L. M. (1990b) Inhibition of calcite growth rates by Mn^{2+} in $CaCl_2$ solutions at 10, 25, and 50°C. *Geochim. Cosmochim. Acta* **54**, 2991–3000.

EMERY D. and MARSHALL J. D. (1989) Zoned calcite cements: Has analysis outpaced interpretation? *Sediment. Geol.* **65**, 205–210.

FAGIOLI R. O., REEDER R. J., MEYERS W. J. (1985) Synthetic cathodoluminescent banding in artificially grown calcite crystals. In *Collected Abstracts, SEPM Ann. Midyear Mtg.* **2**, 28–29.

FAIRCHILD I. J (1983) Chemical controls of cathodoluminescence of natural dolomites and calcites: New data and review. *Sedimentology* **30**, 579–583.

FRAGA, H., GALI S., and FONT ALTABA M. (1982) Sector zoning as a growth phenomenon and its influence in the optical properties of crystals. The case of grossular-andradite garnets. In *Crystal Growth Processes in Sedimentary Environments* (ed. R. RODRÍGUEZ-CLEMENTE and I. SUNAGAWA), Consejo Sup. Invest. Científicas.

FRANK J. R., CARPENTER A. B., and OGLESBY T. W. (1982) Cathodoluminescence and composition of calcite cement in the Tau Sauk Limestone (Upper Cambrian), Southeast Missouri. *J. Sediment. Petrol.* **52**, 631–638.

FRASER D. G., FELTHAM D., and WHITEMAN M. (1989) High-resolution scanning proton microprobe studies of micro-scale trace element zoning in a secondary dolomite: Implications for studies of redox behavior in dolomites. *Sediment. Geol.* **65**, 223–232.

GROVER G. A., JR, and READ J. F. (1983) Paleoaquifer and deep burial related cements defined by regional cathodoluminescent patterns, Middle Ordovician carbonates, Virginia. *AAPG. Bull.* **67**, 1275–1303.

HAASE C. S., CHADAM J., FEINN D., and ORTOLEVA P. (1980) Oscillatory zoning in plagioclase feldspar. *Science* **209**, 272–274.

HAYES K. F. and LECKIE J. O. (1986) Mechanism of lead ion adsorption at the goethite-water interface. In *Geochemical Processes at Mineral Surfaces* (ed. J. A. DAVIS and K. F. HAYES) pp. 114–141. American Chemical Society.

HELGESON H. C., MURPHY W. M., and AAGAARD P. (1984) Thermodynamic and kinetic constraints on reaction rates among minerals and aqueous solutions. II. Rate constants, effective surface area, and the hydrolysis of feldspar. *Geochim. Cosmochim. Acta* **48**, 2405–2432.

HENRY D. J., TONEY J. B., SUCHEKI R. K., and BLOCH S. (1986) Development of quartz overgrowths and pressure solution in quartz sandstones: Evidence from cathodoluminescence and back-scattered electron imaging and trace element analysis on the electron microprobe. *GSA Abstr. Prog.* **18**, 635.

HLAVÁČEK V., KUBÍČEK M., and MAREK M. (1969) Analysis of nonstationary heat and mass transfer in a porous catalyst particle. *J. Catalysis* **15**, 17–30.

HONEYMAN B. D. and LECKIE J. O. (1986) Macroscopic partitioning coefficients for metal ion adsorption: Proton stoichiometry at variable pH and adsorption density. In *Geochemical Processes at Mineral Surfaces* (ed. J. A. DAVIS and K. F. HAYES) pp. 162–190, American Chemical Society.

KUANG C. (1989) Kinetic study of dissolution of hedenbergite and grossularite at 200°C. *28th Int. Geol. Congr. Abst.* 2, 236.

LI Y.-H. and GREGORY S. (1974) Diffusion of ions in sea water and in deep-sea sediments. *Geochim. Cosmochim. Acta* **38**, 703–714.

LORENS R. B. (1981) Sr, Cd, Mn, and Co distribution coefficients in calcite as a function of calcite precipitation rate. *Geochim. Cosmochim. Acta* **45**, 553–561.

MASON R. A. (1987) Ion microprobe analysis of trace elements in calcite with an application to the cathodoluminescence zonation of limestone cement from the Lower Carboniferous of South Wales, UK. *Chem. Geol.* **64**, 209–224.

MERINO E. (1979) Internal consistency of a water analysis and uncertainty of the calculated distribution of aqueous species at 25°C. *Geochim. Cosmochim. Acta* **43**, 1533–1542.

MERINO E. (1984) Survey of geochemical self-patterning phenomena. In *Chemical Instabilities* (ed. G. NICOLIS and F. BARAS) pp. 305–328. Reidel.

MEYER H. J. (1984) The influence of impurities on the growth rate of calcite. *J. Crystal Growth* **66**, 639–646.

MEYERS W. J. (1974) Carbonate cement stratigraphy of the Lake Valley Formation (Mississipian), Sacramento Mountains, New Mexico. *J. Sediment. Petrol.* **44**, 837–861.

MEYERS W. J. (1978) Carbonate cements: Their regional distribution and interpretation in Mississipian limestones of southwest New Mexico. *Sedimentology* **25**, 371–400.

MEYERS W. J., GRAMS J. C., and HEMMING N. G. (1988) Covariations of trace elements in Mississippian calcite cements: Implications for CL and causes of zoning. In *Abstracts: Analysis and Interpretation of Zoned Calcite Cements*. Geological Society, London.

MUCCI A. (1988) Manganese uptake during calcite precipitation from seawater: Conditions leading to the formation of pseudokutnahorite. *Geochim. Cosmochim. Acta* **52**, 1859–1868.

NICOLIS G. and PRIGOGINE I. (1977) *Self-Organization in Nonequilibrium Systems*. John Wiley & Sons.

ORTOLEVA P., MERINO E., MOORE C., and CHADAM J. (1987) Geochemical self-organization, I: Reaction-transport feedbacks and modeling approach. *Amer. J. Sci.* **287**, 979–1007.

PARKS G. A. (1975) Adsorption in the marine environment. *Chem. Ocean.* **1**, 241–308.

PIERSON B. J. (1981) The control of cathodoluminescence in dolomite by iron and manganese. *Sedimentology* **28**, 601–610.

PINGITORE N. E., EASTMEN M. P., SANDIDGE M., ODEN K., and FREIDA B. (1988) The coprecipitation of manganese (II) with calcite: An experimental study. *Mar. Chem.* **25**, 107–120.

PLUMMER L. N., WIGLEY T. M. L., and PARKHURST D. L. (1978) The kinetics of calcite dissolution in CO_2-water systems at 5° to 60°C and 0.0 to 1.0 atm CO_2. *Amer. J. Sci.* **278**, 179–216.

REEDER R. J. (1986) Zoning types and their origins in sedimentary carbonate minerals. In *Geochemistry of the Earth's Surface* (ed. R. RODRÍGUEZ and Y. TARDY) pp. 740-752. Consejo Sup. Invest. Cientificas, Centre Nat. Recher. Scientifique.

REEDER R. J. and GRAMS J. C. (1987) Sector zoning in calcite cement crystals: Implications for trace element distribution in carbonates. *Geochim. Cosmochim. Acta* **51**, 187–194.

REEDER R. J., FAGIOLI R. O., and MEYERS W. (1990) Oscillatory zoning of Mn in solution-grown calcite crystals. *Earth Sci. Rev.* **29**, 39–46.

SAMOYLOVICH Y. A. (1979) The possibility of crystallization in an oscillatory mode in a magmatic body. *Geochem. Intl.* **16**, 79–84.

STUMM W. and MORGAN J. J. (1981) *Aquatic Chemistry*. John Wiley & Sons.

STUMM W. and WIELAND E. (1990) Dissolution of oxide and silicate minerals: Rates depend on surface speciation. In *Aquatic Chemical Kinetics* (ed. W. STUMM) pp. 367–400. John Wiley & Sons.

STUMM W., FURRER G., and KUNZ B. (1983) The role of surface coordination in precipitation and dissolution of mineral phases. *Croat. Chem. Acta* **58**, 593–611.

TEN HAVE T. and HEIJINEN W. (1985) Cathodoluminescence activation and zonation in carbonate rocks: An experimental approach. *Geol. Mijinbouw* **64**, 297–310.

WANG Y. and MERINO E. (1990) Self-organizational origin of agates: Banding, fiber twisting, composition, and dynamic crystallization model. *Geochim. Cosmochim. Acta* **54**, 1627–1638.

YASUNAGA T. and IKEDA T. (1986) Adsorption-desorption kinetics at metal-oxide-solution interface studied by relaxation methods. In *Geochemical Processes at Mineral Surfaces* (ed. J. A. DAVIS and K. F. HAYES) pp. 230–253. American Chemical Society.

APPENDIX

Steady States

The steady states of the system of Eqns. (29a and b) are obtained by taking the time derivatives on the left to be zero, and solving for u and v, now designated as u_0, v_0:

$$1 - u_0 - \lambda[1 + \beta_1\gamma(1 - u_0) + \beta_2\gamma(1 - u_0)^2]u_0 = 0, \quad \text{and} \quad (A1)$$

$$v_0 = \gamma(1 - u_0). \quad (A2)$$

Because Eqn. (A1) is cubic, the system may have one or three steady states, depending on λ, β_1, β_2, and γ. Figure 7 indicates that decreases in these parameters reduce the slope of the tangent to $f_1(u)$ at $u = 1$, resulting in three possible steady states. As shown below, the system displays different behaviors around the different steady states.

Linear Stability Analysis about Steady States

Following the standard procedure (HLAVÁČEK et al., 1969; COOK, 1986, pp. 14–43), we introduce small perturbations δu and δv around a steady state (u_0, v_0), and replace

$$u = u_0 + \delta u, \quad v = v_0 + \delta v \quad (A3)$$

into Eqns. (29a and b). Linearizing the equations (that is, keeping only terms linear in δu or δv), we obtain

$$\frac{d\delta u}{d\tau} = \phi_u\delta u + \phi_v\delta v$$

$$\frac{d\delta v}{d\tau} = \psi_u\delta u + \psi_v\delta v, \quad (A4)$$

where $\Phi(u, v) = du/d\tau$, and $\Psi(u, v) = dv/d\tau$, and the subscripts indicate the partial derivatives at the steady state. A general solution to Eqn. (A4) is of the form

$$\delta u = k_1 \exp(\zeta_1\tau) + k_2 \exp(\zeta_2\tau)$$

$$\delta v = k_1' \exp(\zeta_1\tau) + k_2' \exp(\zeta_2\tau), \quad (A5)$$

where k_1, k_2, k_1', and k_2' are integration constants; and ζ_1 and ζ_2 are the roots of the characteristic equation,

$$\zeta^2 - (\phi_u + \psi_v)\zeta + \phi_u\psi_v - \phi_v\psi_u = 0. \quad (A6)$$

The behavior of the system near the steady state can be characterized by ζ_1 and ζ_2 or, equivalently, by the quantities (HLAVÁČEK et al., 1969, p. 20):

$$S = \phi_v\psi_u - \phi_u\psi_v,$$

$$D = (\phi_u - \psi_v)^2 - 4\phi_v\psi_u, \quad \text{and}$$

$$Q = \phi_u + \psi_v. \quad (A7)$$

According to those quantities, the steady states of the system are classified into (HLAVÁČEK et al., 1969, p. 20; COOK, 1986, pp. 20–23):

saddle point $S > 0$

node $S < 0$, $D > 0$,
and $Q < 0$ stable $Q > 0$ unstable

focus $S < 0$, $D < 0$,
and $Q < 0$ stable $Q > 0$ unstable.

The steady states of focus and unstable node are the ones of interest here, for they may bring about oscillatory solutions to Eqns. (29a and b), corresponding to the oscillatory zoning in calcite.

By obtaining the partial derivatives of Φ and Ψ from their definitions, the condition $S < 0$ becomes:

$$-\frac{v_0^2}{\gamma} + v_0 - \frac{1 + \beta_1 v_0 + \beta_2 v_0^2}{\beta_1 + 2\beta_2 v_0} < 0. \quad (A8)$$

Similarly, $D < 0$ and $Q > 0$, respectively, yield:

$$\{\theta + u_0[\gamma\lambda(\beta_1 + 2\beta_2 v_0)u_0 - 1]\}^2 - 4\lambda(\beta_1 + 2\beta_2 v_0)u_0^2 v_0\theta < 0 \quad (A9)$$

$$\theta < \frac{(\beta_2 v_0^2 - 1)u_0}{1 + \beta_1 v_0 + \beta_2 v_0^2} = \theta_c, \quad (A10)$$

where θ_c is the critical value of θ. Similarly, θ satisfying the equality in Eqn. (A9) is denoted by θ_{focus}. Conditions (A8–10) guide us in selecting appropriate parameter values (α, β_1, β_2, γ, and θ) to carry out numerical solutions of the full nonlinear Eqns. (29a and b); these numerical solutions are plotted in Figs. 2–5.